

Neutrino-pair bremsstrahlung in a neutron star crust

D. D. OFENGEIM^{1,2}, A. D. KAMINKER¹ and D. G. YAKOVLEV¹

¹ *Ioffe Institute, Politechnicheskaya 26, 194021, St. Petersburg, Russia*

² *St. Petersburg Academic University, Khlopina Street 8/3, St. Petersburg 194021, Russia*

PACS 13.15.+g – Neutrino interactions

PACS 97.60.-s – Late stages of stellar evolution (including black holes)

PACS 21.65.Cd – Nuclear matter: Asymmetric matter, neutron matter

Abstract –Based on the formalism by Kaminker et al. (Astron. Astrophys. **343** (1999) 1009) we derive an analytic approximation for neutrino-pair bremsstrahlung emissivity due to scattering of electrons by atomic nuclei in the neutron star crust of any realistic composition. The emissivity is expressed through generalized Coulomb logarithm which we fit by introducing an effective potential of electron-nucleus scattering. In addition, we study the conditions at which the neutrino bremsstrahlung in the crust is affected by strong magnetic fields. The results can be applied for modelling of many phenomena in neutron stars, such as thermal relaxation in young isolated neutron stars and in accreting neutron stars with overheated crust in soft X-ray transients.

Introduction. – It is well known that studies of the thermal evolution of neutron stars allows one to explore the physics of their superdense matter [1]. The thermal evolution, in turn, is largely determined by neutrino emission from various neutron star layers [2]. Here we focus on the most important neutrino emission mechanism in the neutron star crust, which is the emission of neutrino-antineutrino pairs (of any flavors, through charged and neutral electroweak currents) in collisions of electrons (e) with atomic nuclei (A, Z). It is also called the neutrino-pair bremsstrahlung, written schematically as

$$e + (A, Z) \rightarrow e + (A, Z) + \nu + \bar{\nu}. \quad (1)$$

It was proposed by Pontecorvo [3] and has been studied in astrophysical context many times as reviewed in [2].

We employ the formalism of [4] which includes the most complete collection of physical effects important in (1) and allows one to calculate the neutrino bremsstrahlung emissivity Q [erg s⁻¹ cm⁻³] for any composition of neutron star crust. To use these results in modeling of neutron star phenomena, one needs either extensive tables or analytic fits of Q . The authors of [4] fitted Q for the ground-state crust. However, the composition may differ from the ground state; for instance, the crust can be accreted [1]. Accordingly, one needs to fit Q for a wide range of possible compositions. In this Letter we calculate Q for different compositions and obtain the required fit. In addition, we investigate the conditions at which the process (1) is affected by magnetic fields.

Formalism. – We analyze the process (1) in the crust of a neutron star without magnetic field (but we discuss the magnetic effects in the end of the Letter). Under the crust we mean the envelope of the star which contains atomic nuclei. It extends [1] to the density $\rho \approx 1.5 \times 10^{14}$ g cm⁻³, about half of the saturated nuclear matter density. The atomic nuclei there are crystallized or form Coulomb liquid.

At any value of ρ the matter is assumed to contain spherical atomic nuclei of one species. The nuclei are immersed in the sea of electrons, and at densities higher than the neutron drip density $\rho_{\text{ND}} \approx (4 - 6) \times 10^{11}$ g cm⁻³ [2], also in the sea of free neutrons.

Following [4] we will restrict ourselves to the case of ultrarelativistic and strongly degenerate electrons. In this case $p_F \gg m_e c$, that is $\rho \gg 10^6$ g cm⁻³, where $p_F = \hbar(3\pi^2 n_e)^{1/3}$ is the electron Fermi momentum, m_e the electron rest-mass, and n_e is the electron number density. Such electrons are strongly degenerate at $cp_F \gg k_B T$, T being the temperature and k_B the Boltzmann constant. Under these conditions the electrons form nearly ideal Fermi gas and the nuclei (ions) are fully ionized by the electron pressure. The electric neutrality of the matter implies $n_e = Zn_i$, where n_i is the number density of the nuclei, and Z is the nucleus charge number. Let us introduce also A_{tot} , the total number of nucleons per one nucleus, and $A = A_{\text{nuc}}$, the total number of nucleons confined in one nucleus. In the outer crust ($\rho < \rho_{\text{ND}}$) we have $A_{\text{tot}} = A$, while in the inner crust ($\rho \geq \rho_{\text{ND}}$) one

gets $A_{\text{tot}} > A$ (with $A_{\text{tot}} - A$ being the number of free neutrons per one nucleus). The mass density of the matter in the crust is $\rho \approx m_u A_{\text{tot}} n_i$, where m_u is the atomic mass unit.

Let us introduce the dimensionless parameters

$$x = \frac{p_F}{m_e c} = 25.73 (Z n_{i34})^{1/3}, \quad (2)$$

$$\Gamma = \frac{Z^2 e^2}{k_B T a} = 0.5798 \frac{Z^2}{T_9} n_{i34}^{1/3}, \quad (3)$$

$$\tau = \frac{T}{T_{\text{pi}}} = 0.9914 \frac{T_9}{Z} \sqrt{\frac{A}{n_{i34}}}, \quad (4)$$

$$\xi = \frac{R_p p_F}{\hbar} = \left(\frac{9\pi}{4} Z \right)^{1/3} \frac{R_p}{a} \\ = 0.06665 R_{p \text{ fm}} (Z n_{i34})^{1/3}. \quad (5)$$

Here $a = (4\pi n_i)^{-1/3}$ is the ion sphere (spherical Wigner-Seitz cell) radius; $T_{\text{pi}} = \hbar \omega_{\text{pi}} / k_B$ is the ion plasma temperature determined by the ion plasma frequency $\omega_{\text{pi}} = \sqrt{4\pi Z^2 e^2 n_i / (A m_u)}$; $n_{i34} = n_i / (10^{34} \text{ cm}^{-3})$; $T_9 = T / (10^9 \text{ K})$; $R_{p \text{ fm}} = R_p / (1 \text{ fm})$ is the proton core radius of the nucleus expressed in fm. Thus, x is the relativity parameter of degenerate electrons ($x \gg 1$ in our case); Γ is the Coulomb coupling parameter ($\Gamma \lesssim 1$ for ion gas; $\Gamma \gtrsim 1$ for ion liquid or crystal; crystallization occurs at $\Gamma = 175$); τ determines the importance of quantum effects in ion motion; ξ specifies the importance of finite sizes of the nuclei; see [1] for details.

According to [4], the emissivity of the process (1) is

$$Q = \frac{8\pi G_F^2 e^4 C_+^2}{567 \hbar^9 c^8} Z^2 (k_B T)^6 n_i L(Z, A, R_p, n_i, T) R_{\text{NB}} \\ = 5.362 \times 10^{15} Z^2 n_{i34} T_9^6 L R_{\text{NB}} \text{ erg cm}^{-3} \text{ s}^{-1}. \quad (6)$$

Here G_F is the Fermi weak interaction constant; $C_+^2 = 1.675$ takes into account three neutrino flavors; $R_{\text{NB}} = 1 + 0.00554Z + 0.0000737Z^2$ is an approximate non-Born correction. Furthermore, L is the generalized Coulomb logarithm to be determined; $L = L_{\text{liq}}$ in the liquid phase; $L = L_{\text{ph}} + L_{\text{sl}}$ in the solid phase, where L_{ph} is the contribution of electron-phonon scattering, and L_{sl} is the contribution of Bragg diffraction of electrons on the static lattice. In the liquid phase,

$$L_{\text{liq}} = \int_0^1 S_{\text{liq}}(q) |V(q)|^2 \mathcal{R}_c(y) y^3 dy, \quad (7)$$

where $\hbar q$ is the electron momentum transfer in a reaction event and $y = \hbar q / (2p_F)$. The function $S_{\text{liq}}(q)$ is the ion structure factor in the Coulomb liquid [5]; it takes into account ion-ion correlations which introduce strong ion screening of the electron-nucleus interaction; $\mathcal{R}_c(y) = 1 + 2y^2 (\ln y) / (1 - y^2)$ comes from the squared matrix element; $V(q) = F(q) / (y^2 + y_0^2)$ is the Fourier transform of the Coulomb potential screened by electron polarization (included into y_0 [4]); $F(q)$ is the nuclear form

factor which takes into account proton charge distribution within the nucleus and associated additional effective screening [4].

Let us consider the proton charge distribution within the nucleus as uniform (uniformly charged sphere of radius R_p). Then $F(q) = F(u) = 3(\sin u - u \cos u) / u^3$, $u = 2\xi y$. At $\rho \lesssim 10^{12} \text{ g cm}^{-3}$ one typically has $R_p \ll a$ and finite sizes of atomic nuclei are unimportant. Then it is sufficient to set $R_p \rightarrow 0$ ($\xi \rightarrow 0$, $F(q) = 1$), i.e., treat the nuclei as point-like. At $\rho \gtrsim 10^{12} \text{ g cm}^{-3}$, the nuclei occupy a non-negligible volume which introduces extra effective screening of the electron interaction with the nuclei. In the density range $10^{12} \lesssim \rho \lesssim 10^{13} \text{ g cm}^{-3}$ the approximation of uniformly charged proton core is reasonably good but at higher ρ it breaks down (the proton cores are greatly broadened by the density effects [1]). However, in this case one can take realistic proton charge distribution, calculate its root-mean-square value, $\sqrt{\langle R_p^2 \rangle}$, and use this value instead of R_p in the formulas obtained formally for the uniform charge distribution. This turns out to be a good approximation [6] which allows us to use the employed formalism even if real nuclei are charged non-uniformly.

The expression for L_{ph} is

$$L_{\text{ph}} = \int_{(4Z)^{-1/3}}^1 S_{\text{ph}}(q) |V(q)|^2 \mathcal{R}_c(y) y^3 dy. \quad (8)$$

An appropriate effective structure factor S_{ph} is obtained in [7] and takes into account multiphonon processes,

$$S_{\text{ph}} = [\exp(w_1 y^2) - 1] \exp(-w y^2), \quad (9)$$

$$w_1 = (12\pi^2)^{1/3} \frac{Z^{2/3} u_{-2}}{\Gamma} \frac{b\tau}{\sqrt{(b\tau)^2 + u_{-2}^2 \exp(-7.6\tau)}}, \quad (10)$$

$$w = (12\pi^2)^{1/3} \frac{Z^{2/3} u_{-2}}{\Gamma} \left(\frac{u_{-1}}{2u_{-2}} \frac{\exp(-9.1\tau)}{\tau} + 1 \right), \quad (11)$$

where $b = 231$, $u_{-1} = 2.798$, and $u_{-2} = 12.972$ (u_{-1} and u_{-2} being dimensionless moments of phonon frequencies of the Coulomb crystal). The crystal is assumed to have the body centered cubic structure, but the results are fairly insensitive to the lattice type [4].

Finally,

$$L_{\text{sl}} = \frac{1}{12Z} \sum_{\mathbf{K} \neq 0} (1 - y^2) y^2 |V(\mathbf{K})|^2 I(t_V, y) \exp(-w y^2), \quad (12)$$

where \mathbf{K} is a reciprocal lattice vector, $y = \hbar |\mathbf{K}| / (2p_F)$,

$$\frac{1}{t_V} = \frac{\Gamma}{Z} \left(\frac{4}{3\pi Z} \right)^{2/3} \sqrt{1 - y^2} |V(\mathbf{K})| \exp(-w y^2). \quad (13)$$

The function $I(t_V, y)$ has been analyzed in [4]; it takes into account electron band structure effects (Bloch states instead of plain waves). These effects broaden Bragg diffraction peaks and reduce L_{sl} [8].

Note that the approach [4] does not take into account the quantum effects of ion motion in the liquid state [$S_{\text{liq}}(q)$ in (7) is classical, independent of τ]. This approximation may actually be violated, especially for light ions near the melting point. However, for heavy ions the approximation is justified at all T in the liquid. Note also that in our case L is explicitly independent of x .

We will calculate and fit the Coulomb logarithm $L(Z, A, R_p, n_i, T)$. It can be presented as a function of four dimensionless arguments, $L = L(Z, \Gamma, \tau, \xi)$.

Coulomb logarithm and effective potential. – Our fit of the Coulomb logarithm will use the concept of effective potential for the electron-nucleus scattering in the process (1). Similar effective potentials have been introduced by A. Y. Potekhin to fit Coulomb logarithms [6] for electric and thermal conductivities of electrons due to electron-ion (electron-phonon) scattering in the crust. Although the principal approach will be the same, the effective potentials are naturally different.

In our case V_{eff} is introduced as

$$L = \int_0^1 |V_{\text{eff}}(y)|^2 \mathcal{R}_c(y) y^3 dy, \quad |V_{\text{eff}}|^2 = S_{\text{eff}}(y) \frac{|F(2\xi y)|^2}{y^4}, \quad (14)$$

where S_{eff} is the effective structure factor which we present in the form close to (9),

$$S_{\text{eff}} = [\exp(w_1^* y^2) - 1] \exp(-w^* y^2). \quad (15)$$

Then w_1^* and w^* can be taken similar to (10) and (11),

$$w_1^* = B \frac{b\tau_*}{\sqrt{(b\tau_*)^2 + u_{-2}^2 \exp[-7.6(\tau_* + 18/\Gamma_*)]}}, \quad (16)$$

$$w^* = B \left[1 + \frac{u_{-1}}{2u_{-2}\tau_*} \exp\left(-9.1 \left\{ \tau_* + \frac{216}{\Gamma_*} \right\} \right) \right], \quad (17)$$

$$B = \frac{3}{5} \frac{(12\pi^2)^{1/3} u_{-2} Z^{4/5}}{1 + (\xi/Z)\Gamma_*/(200 + \Gamma_*)} \times \left(\Gamma_*^2 + \frac{1037}{(1 + \Gamma_*/204)^4} \frac{\Gamma_*^{(1+0.15\xi)/2}}{Z^{0.10}} \right)^{-1/2}. \quad (18)$$

Here τ_* and Γ_* are rescaled τ and Γ , respectively. They are related to original Γ , τ , ξ and Z as

$$\tau_* = 0.095 \left(\frac{2\tau}{0.095\sqrt{\tau^2 + 4}} \right)^{1/\Lambda}, \quad \Lambda = 1 + \frac{(Z/35.5)^2}{1 + \Gamma/(223Z)}, \quad (19)$$

$$\Gamma_* = \Gamma \exp \left\{ -\frac{\tau_*^{0.053} (Z/11.3)^{4/9}}{1 + \tau_*^G [\Gamma/(19.3Z^{1.7})]^H} \right\}, \quad (20)$$

with $G = 0.5 + 0.002Z\xi$ and $H = [1.52 + 0.9(1 - \tau_*)]/(1 + 0.5\xi)$.

In the high- Γ limit at $\xi = 0$ equations (16) and (17) reduce to (10) and (11), respectively, except that $Z^{2/3}$ transforms to $(3/5)Z^{4/5}$.

For an analytic integration of the Coulomb logarithm (14) we suggest to approximate \mathcal{R}_c as $\mathcal{R}_c(y) \approx 1 - y$ (with a maximum relative error equal to 0.08 at $y = 0.3$ over $0 \leq y \leq 1$) and the form factor as $|F(u)|^2 \approx \exp(-\alpha u^2)$ with $\alpha = 0.23$ (maximum absolute error equal to 0.032 at $u = 1.6$ for any $u \geq 0$). Then (14) takes the form

$$L = f(w^* + 4\alpha\xi^2) - f(w^* - w_1^* + 4\alpha\xi^2), \quad (21)$$

$$f(x) = \frac{1}{2} \left[\sqrt{\frac{\pi}{x}} \operatorname{erf}(\sqrt{x}) + \ln(x) - \operatorname{Ei}(-x) \right],$$

where $\operatorname{erf}(x)$ and $\operatorname{Ei}(x)$ are the standard error function and exponential integral, respectively. Note that $f(x) = 0.71139 + x/6$ as $x \rightarrow 0$.

To clarify the proposed fit let us note that L_{ph} roughly reproduces the full Coulomb logarithm L (fig. 1). Accordingly, L_{ph} is basic for our fit. Modified w^* and w_1^* allow us to accurately reproduce L_{liq} , while Γ_* and τ_* tune the fit of L_{sl} . More details are given below.

The fit contains a number of coefficients which have been initially chosen “by eye” but have been optimized afterwards by comparing with calculations based on the formalism [4]. The comparison has been made on the following grid of the parameters: $Z = 6, \dots, 50$ (10 points), $A = 1.9Z, \dots, 3Z$ (10 points), $R_p = (0.0, \dots, 0.2) \times a$ (10 points), $\log n_i [\text{cm}^{-3}] = 29, \dots, 34$ (15 points), and $\log T [\text{K}] = 8, \dots, 9$ (15 points). Also, we have excluded the cases in which $Q < 10^7 \text{ erg cm}^{-3} \text{ s}^{-1}$ and/or $|\log \Gamma/175| < 0.2$. The first condition excludes the range of parameters where the neutrino bremsstrahlung is too slow (unimportant for applications). The second condition excludes narrow temperature intervals near the melting points. In these intervals the formalism [4] gives relatively small jumps of Q which are believed to be artificial, insignificant for applications and caused by neglecting the quantum effects in ion motion in the liquid phase (see above). Our exclusion condition smoothes out such jumps which seems adequate to the physics of the problem. After these exclusions, the optimization has been provided on 172550 grid points by comparing the values of L , calculated via (7)–(12), with those given by the fits (16)–(21).

After the optimization the root-mean-square relative error of fitted L becomes 8%, with the maximum error $\sim 50\%$ at $Z = 11$, $A = 21$, $n_i = 10^{34} \text{ cm}^{-3}$, $T = 10^8 \text{ K}$, and $R_p = 0.022 a$, in which case $L = 0.059$. This fit accuracy is quite sufficient for applications.

By way of illustration, in fig. 1 we show the dependence of the full Coulomb logarithm L (thick lines) and its partial phonon contribution L_{ph} (thin lines) versus Γ for $\tau = 1$. We present three cases of $Z = 6$ (solid lines) and 26 (short-dashed lines) at $\xi = 0$ (approximation of point-like nuclei, typical for the outer crust) and $Z = 50$ at $\xi = 2$ (finite-size nuclei, characteristic for the bottom of the inner crust). The lines are calculated using the formalism [4]. The kink of the solid line for $Z = 6$ occurs at the melting point because [4] neglects the quantum effects of ion motion in the liquid ($\Gamma < 175$). For the nuclei

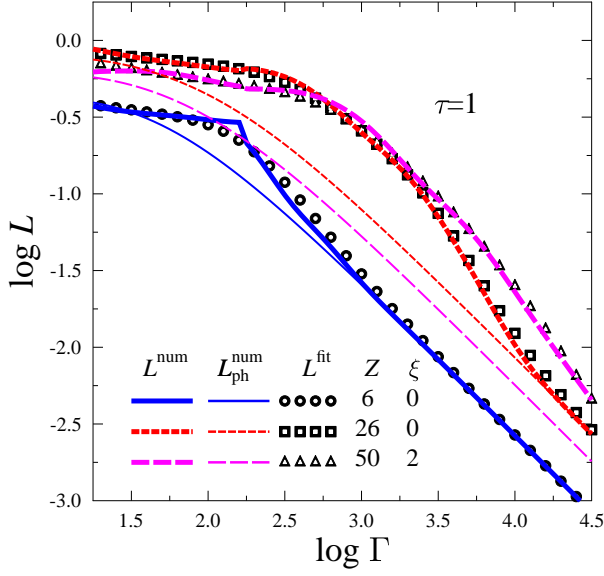


Fig. 1: (Color online) Coulomb logarithms versus Γ in log-log scale at $\tau = 1$ for three types of nuclei. Shown are the full logarithm L^{num} (thick lines) and its formal phonon contribution $L_{\text{ph}}^{\text{num}}$ (thin lines) calculated numerically using the formalism [4], as well as our fits L^{fit} to the full logarithm (symbols). The solid lines and open dots refer to the nuclei with $Z=6$ at $\xi = 0$; the short-dashed lines and squares are for $Z = 26$ and $\xi = 0$, while the long-dashed lines and triangles are for $Z=50$ at $\xi = 2$. See text for details.

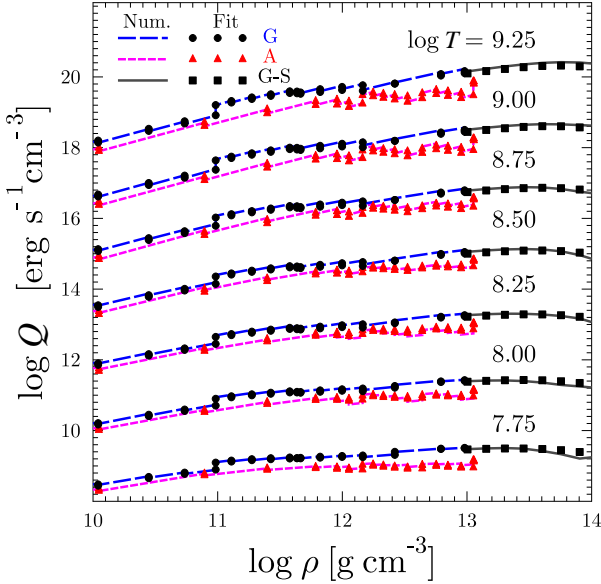


Fig. 2: (Color online) Density dependence of neutrino bremsstrahlung emissivity Q for ground-state (G) and accreted (A) crusts of neutron star at seven temperatures, $T = 10^{7.75}, 10^8, \dots, 10^{9.25}$ K. Lines are calculated using the formalism [4], while symbols are our fits. At $\rho \gtrsim 10^{13}$ g cm $^{-3}$ the smooth composition model of ground-state matter (G-S) is used (see text for details).

with larger Z the quantum effects in the liquid phase are markedly weaker and the kink is smoothed out. Although formally L_{ph} is valid in the crystal, we extend the curve in the liquid. Indeed, as already mentioned before, L_{ph} reasonably well approximates the full Coulomb logarithm in the solid and liquid phases excluding the neighborhood of the melting point.

In the same fig. 1 we plot our fits to the full Coulomb logarithm L (by dots, squares and triangles for $Z = 6, 26$ and 50 , respectively). The quality of the fits is seen to be quite satisfactory.

Figure 2 displays the neutrino emissivity Q as a function of density ρ in the neutron star crust at seven temperatures, $T = 10^{7.75}, 10^8, \dots, 10^{9.25}$ K. We use two models of the crust, the ground-state and accreted one [1,9]. The ground-state crust corresponds to the matter in thermodynamic equilibrium. The accreted crust is formed by nuclear transformations in the matter compressed under the weight of newly accreted material [9]. The numerical values of Q for the ground-state crust are shown by the long-dashed lines, and for the accreted crust by the short-dashed lines. The fits are plotted by filled dots and triangles, respectively. The accreted crust is composed of lighter nuclei with lower Z . The bremsstrahlung neutrino emission in the accreted crust is somewhat lower than in the ground-state one because of lower Z in the accreted crust. In both cases it is assumed that only the nuclei of one type are present at any given density. Slight jumps of the calculated and fitted Q values at some densities are associated with the change of nuclides in dense matter with growing ρ [1]. Our fits reproduce numerically calculated Q values quite well.

At $\rho \gtrsim 10^{13}$ g cm $^{-3}$ the accreted crust becomes almost indistinguishable from the ground-state one, and we do not plot the data for the accreted crust at higher densities. However, the emissivity Q for the dense ground-state crust starts to depend on the proton density profiles within the nuclei (see above). To demonstrate the quality of our fits in this regime we use the smooth-composition model of the ground-state crust at $\rho \gtrsim 10^{13}$ g cm $^{-3}$ (the solid lines), calculate the root-mean-squared proton core radii and use them in our fits (squares). Again, there is good agreement of the theory and fits, just as for kinetic properties of crustal matter [6].

Effects of magnetic fields. — Many neutron stars possess strong magnetic fields which affect various neutrino processes, including the process (1). Accurate calculation of Q for the process (1) is a difficult and still unsolved problem. Here we formulate the conditions at which magnetic fields can modify the process. Evidently, the process can be affected by magnetic fields through electrons and atomic nuclei.

Electrons. A field \mathbf{B} changes the motion of electrons because of Landau quantization of electron states; e.g. [1]. In our case of strongly degenerate relativistic electrons the importance of magnetic effects is mostly determined by the

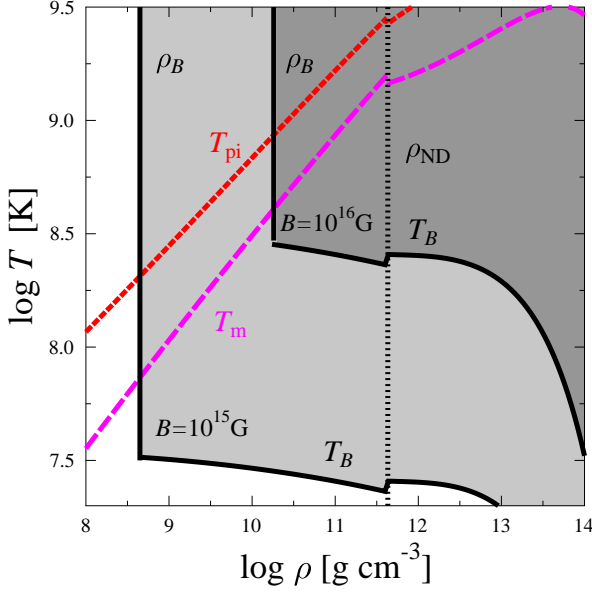


Fig. 3: (Color online) Density-temperature diagram for the ground-state neutron star crust. The densely shaded region is expected to be almost unaffected by the magnetic field $B = 10^{16}$ G, while weakly shaded region is almost unaffected by the field $B = 10^{15}$ G. Any region is bounded by the density ρ_B below which the electrons occupy only the ground Landau level, and by the temperature T_B below which phonon frequencies of Coulomb crystals of atomic nuclei are affected by B . Also shown is the neutron drip density $\rho_{ND} \approx 4.3 \times 10^{11} \text{ g cm}^{-3}$, the melting temperature T_m of the crystal and the ion plasma temperature T_{pi} (see text for details).

characteristic density

$$\rho_B \approx 7045 (A_{\text{tot}}/Z) B_{12}^{3/2} \text{ g cm}^{-3}, \quad (22)$$

where $B_{12} = B/10^{12} \text{ G}$. At $\rho \lesssim \rho_B$ the electrons are strongly quantized (occupy the ground Landau level) while at $\rho \gg \rho_B$ they populate many Landau levels.

Accordingly, we expect that the field B strongly affects the process (1) at $\rho \lesssim \rho_B$. At higher $\rho \gtrsim \rho_B$ the field affects the electron motion much weaker. Such effects are regulated by the characteristic temperature $T_{Be} = \hbar\omega_{Be}/k_B$ associated with gyrofrequency of degenerate electrons, $\omega_{Be} = eB/(m_e c \sqrt{1+x^2})$. If $T \gtrsim T_{Be}$ the thermal broadening of the Landau levels exceeds the spacing between the levels and washes out the Landau level structure. Then the magnetic fields can be treated as non-quantizing; their effects on the process (1) should be weak. At $\rho \gtrsim \rho_B$ but $T \ll T_{Be}$ the thermal broadening of Landau levels is smaller, the structure of the Landau levels may be pronounced, and the magnetic field behaves as weakly quantizing. It may produce not very pronounced quantum oscillations of Q with increasing ρ due to population of higher Landau levels. The emissivity Q averaged over oscillations is expected to resemble the field-free Q . Note that Landau levels can also be broadened by electron

collisions and other delicate effects [10], so that exact calculation of Q can be complicated. However, the magnetic effects of the electrons on Q at $\rho \gtrsim \rho_B$ cannot be dramatic (can be neglected in the first-order approximation).

Atomic nuclei. Strong magnetic fields affect vibration properties (phonon modes) of Coulomb crystals of atomic nuclei and modify the neutrino-pair bremsstrahlung in this way. Phonon modes of magnetized Coulomb crystals have been studied in a number of works, e.g. [11, 12] and references therein. There are three branches of phonon spectrum; all of them can be affected by magnetic fields. Various phonon modes are affected in certain ranges of ρ and T (similar to those plotted in fig. 6 of [12], where magnetic fields modify phonon heat capacity). These effects are mostly pronounced at

$$T \ll T_B = \frac{\hbar\omega_B}{k_B}, \quad \omega_B = \frac{ZeB}{A_{\text{nuc}}m_{\text{uc}}}, \quad (23)$$

where ω_B is the ion cyclotron frequency. It is natural to expect that at $T \gtrsim T_B$ the process (1) is not affected by magnetic fields through the ion motion.

Figure 3 shows possible ranges of ρ and T in the neutron star crust where magnetic fields can influence the neutrino-pair bremsstrahlung for the smooth-composition model of the ground-state matter. We expect that the densely shaded region is not affected by the magnetic field $B = 10^{16}$ G, whereas the slightly shaded region is not affected by the field $B = 10^{15}$ G. Any of these two regions is bounded by the density ρ_B , equation (22), and by the temperature T_B , equation (23). We see that the fields $B \lesssim 10^{15}$ G have practically no effects on neutrino-pair bremsstrahlung in the neutron star crust under formulated conditions (see above), while higher fields may affect this neutrino process, especially at low densities.

In addition, in fig. 3 we plot the neutron drip density $\rho_{ND} \approx 4.3 \times 10^{11} \text{ g cm}^{-3}$, the melting temperature T_m of the crystal and the ion plasma temperature T_{pi} for the ground state matter. All these quantities are presented neglecting the effects of magnetic fields.

Conclusions. – Using the formalism [4], which includes rich spectrum of physical effects, we have derived a universal fit for the neutrino emissivity Q of electron-nucleus bremsstrahlung (1) in a neutron star crust (envelope). We have fitted the expression for the generalized Coulomb logarithm L which determines Q . To this aim, we have used the method of effective potential V_{eff} of the electron-nucleus interaction and proposed its form (14).

We expect that our fit is valid for any realistic composition of the neutron star crust, whereas the fit presented in [4] is obtained only for the ground-state crust. Our fit is thought to be accurate in wide ranges of parameters, particularly, in the density range from about 10^8 g cm^{-3} to the crust bottom and in a wide temperature range (from about a few times of 10^7 K to a few times of 10^9 K). It is valid for the nuclei with $6 \lesssim Z \lesssim 50$ and $1.9Z \lesssim A_{\text{nuc}} \lesssim 3Z$. The fit is convenient for using in

computer codes which simulate thermal evolution of neutron stars. The fit assumes the presence of nuclei of one type at any values of ρ and T . In the case of multicomponent plasma we recommend to use the approach of mean nucleus (mean ion), e.g. [1].

As already mentioned before, the process (1) is the leading neutrino process in a neutron star crust. It is important for modelling transient phenomena in warm neutron stars. These phenomena are associated with powerful processes of energy release in the crust and/or thermal relaxation of the crust and core. In particular, we mean thermal relaxation in young (age 10–100 yr) isolated neutron stars [6, 13]; thermal relaxation in accreting neutron stars with overheated crust in soft X-ray transients (after accretion stops and the crust equilibrates with the core, as observed in MXB 1659–298, KS 1731–260 and some other sources, e.g. [14, 15] and references therein). The process (1) can also be important in X-ray superbursts in accreting neutron stars (e.g. [16] and references therein), and in thermal evolution of magnetars in quasistationary and bursting states [17]. In many cases the composition of the crust is variable which affects the neutrino emission and should be taken into account. In addition, there could be isolated cooling neutron stars which are strongly superfluid inside. Superfluidity suppresses the main neutrino processes in stellar cores and makes neutrino emission from the crust important for global thermal evolution [18].

Our results can also be important for massive cooling white dwarfs (or proto white dwarfs) or other stars with massive degenerate cores (red giants and supergiants).

Although our results seem useful for many applications, the theory of the process (1) needs to be elaborated. First, it would be interesting to consider the process (1) in a multicomponent plasma of atomic nuclei which would require complicated calculations of corresponding structure factors. Second, one needs to include the quantum effects of ion motion in the ion liquid which is the long-standing but still unsolved problem. Third, it would be important to study (1) for the electron gas of any relativity and degeneracy; this can be done but requires a lot of effort. Fourth, it would be interesting to analyze the process (1) in possible phases of nuclear pasta of highly non-spherical nuclear clusters which can exist in a layer between the neutron star crust and the core. The latter problem requires the Debye-Waller factors for such clusters [4] which are currently unavailable. Finally, it would be important to take into account the effects of strong magnetic fields in neutron stars. We have analysed the conditions at which very strong fields can affect the process (1) but the influence of the field on the process is still not explored and seems to be a technically complicated task. The consideration of all these problems goes far beyond the scope of this paper.

* * *

This work was supported by the Russian Science Foundation, grant 14-12-00316.

REFERENCES

- [1] HAENSEL P., POTEKHIN A. Y., and YAKOVLEV D. G., *Neutron stars 1: Equation of State and Structure* (Springer, New York) 2007.
- [2] YAKOVLEV D. G., KAMINKER A. D., GNEDIN O. Y. and HAENSEL P., *Phys. Rep.*, **354** (2001) 1.
- [3] PONTECORVO B., *Zh. Eksper. Teor. Fiz.*, **36** (1959) 1615 (English transl. Sov. Phys. JETP **9** (1959) 1148).
- [4] KAMINKER A. D., PETHICK C. J., POTEKHIN A. Y., THORSSON V., and YAKOVLEV D. G., *Astron. Astrophys.*, **343** (1999) 1009.
- [5] YOUNG D. A., COREY M. E., and DEWITT H. E., *Phys. Rev. A*, **44** (1991) 6508.
- [6] GNEDIN O. Y., YAKOVLEV D. G., and POTEKHIN A. Y., *MNRAS*, **324** (2001) 725.
- [7] BAIKO D. A., KAMINKER A. D., POTEKHIN A. Y., and YAKOVLEV D. G., *Phys. Rev. Lett.*, **81** (1998) 5556.
- [8] PETHICK C. J. AND THORSSON V., *Phys. Rev. D*, **56** (1997) 5748.
- [9] HAENSEL P. and ZDUNIK J. L., *Astron. Astrophys.*, **229** (1990) 117.
- [10] SHOENBERG D., *Magnetic Oscillations in Metals* (Cambridge University Press, Cambridge) 1984.
- [11] BAIKO D. A., *Phys. Rev. E*, **80** (2009) 046405.
- [12] BAIKO D. A. and YAKOVLEV D. G., *MNRAS*, **433** (2013) 2018.
- [13] LATTIMER J. M., VAN RIPER K. A., PRAKASH M., and PRAKASH M., *Astrophys. J.*, **425** (1994) 802.
- [14] DEGENAAR N. ET AL., *Astrophys. J.*, **775** (2013) 48.
- [15] DEGENAAR N., WIJNANDS R., and MILLER J. M., *Astrophys. J.*, **767** (2013) L31.
- [16] GUPTA S., BROWN E. F., SCHATZ H., MÖLLER P., and KRATZ K.-L., *Astrophys. J.*, **662** (2007) 1188.
- [17] MEREGHETTI S., *Braz. J. Phys.*, **43** (2013) 356.
- [18] YAKOVLEV D. G., KAMINKER A. D., and GNEDIN, O. Y., *Astron. Astrophys.*, **379** (2001) L5.